An Experimental And Numerical Study Of Elastic Strain Waves On The Center Line Of A 6061-T6 Aluminum Bar

J. L. Habberstad

K. G. Hoge

J. Earl Foster
Missouri University of Science and Technology

J. L. HABBERSTAD[2]
Assoc. Mem. ASME

K. G. HOGE
Lawrence Radiation Laboratory,
University of California,
Livermore, Calif.

J. E. FOSTER
Engineering Mechanics Department,
University of Missouri,
Rolla, Mo.

An Experimental and Numerical Study of Elastic Strain Waves on the Center Line of a 6061-T6 Aluminum Bar[1]

The elastic strain waves resulting from the impact of two 3/4-in-dia 6061-T6 aluminum bars are studied experimentally and analytically. Experimental data are obtained from strain gages on the center line and outer surface of the bar, located at various distances from the impact end of the bar. Experimental data are compared to numerical results obtained from integrating the exact equations of two-dimensional motion. In general, agreement between the numerical and experimental results is very good.

Introduction

A considerable amount of effort has been expended in recent years in developing two-dimensional analytical and numerical techniques. Much of this effort has been directed toward understanding wave motion in axisymmetric bars with various boundary and initial conditions.

The first major contribution to this field was made by Pochammer [1][3] in 1876 and independently by Chree [2] in 1889. They obtained a solution for axisymmetric motion in an infinitely long bar having a free radial surface. This solution points out the dispersive effects that occur in the bar as a result of the presence of the radial surface. Numerical values for Pochammer's and Chree's frequency equation were obtained by Bancroft [3]. Davies [4] noted an error in Bancroft's work and extended the numerical results. Bertholf [5] programmed the frequency equation on an IBM 709 computer and obtained good correlation with Davies' published values.

The introduction of end conditions on the bar complicates the mathematics required to obtain an analytic solution. For this reason, such a solution was not obtained until 1957 when Skalak [6] analyzed the elastic collision of two isotropic semi-infinite bars using a superposition technique. Folk, et al. [7] studied the case of a pressure shock applied to a radial constrained end of a semi-infinite bar. Jones and Norwood [8] extended this solution. Kennedy and Jones [9] solved this same problem but allowed the pressure to vary as a function of the radial position on the end of the bar. In all the foregoing solutions, the resulting integrals are so complicated that to date only asymptotic evaluation of the solution at large distances from the end of the bar has been accomplished.

A large quantity of two-dimensional numerical work has been done over the last few years, much of it based on a velocity formulation utilizing the conservation of mass, momentum, and energy. This formulation requires the introduction of an artificial viscosity term in the manner suggested by the work of von Neumann and Richtmyer [10]. Examples of this type of scheme applied to two-dimensional problems are contained in the works of Wilkins [11], Thorne and Herrmann [12], and Hanagud, et al. [13].

By using the equilibrium equation in conjunction with Hooke's law, one can obtain in terms of displacement components a set of differential equations which govern axisymmetric motion in a bar. Bertholf [14] showed that these equations can be integrated numerically without the explicit introduction of an artificial viscosity term. This numerical procedure has since been expanded by Kennedy and Jones [9] and Habberstad [15].

To date, attempts to correlate the analytical and two-dimensional numerical solutions with experimental data have been restricted to a comparison of strain and radial displacement effects measured on the free radial surface of the bar. Examples of such work can be found in many of the previously cited references. It is our intention to compare numerical and experimental axial strain results not only on the free surface, but also on the center line of a metal bar.

A limited amount of work has been done on internal strain measurement, e.g., Baker and Dove [16] and Meitzler [17].

[1] Work performed under the auspices of the U. S. Atomic Energy Commission.

[2] Now at Bureau of Mines Research Lab, Spokane, Wash.

[3] Numbers in brackets designate References at end of paper.

Contributed by the Applied Mechanics Division and presented at the Applied Mechanics Western Conference, University of Southern California, Los Angeles, Calif., August 23–25, 1971, of The American Society of Mechanical Engineers.

Discussion on this paper should be addressed to the Editorial Department, ASME, United Engineering Center, 345 East 47th Street, New York, N. Y. 10017, and will be accepted until July 20, 1972. Discussion received after the closing date will be returned. Manuscript received by ASME Applied Mechanics Division, November 6, 1970. Paper No. 71-APMW-22.

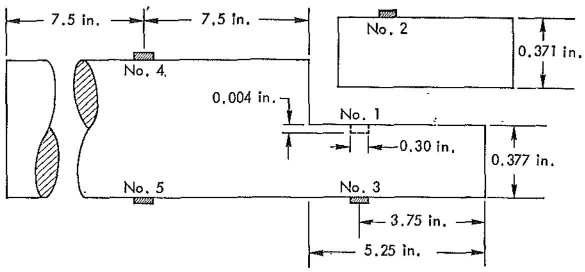

Fig. 1 Test bar configuration showing strain-gage locations

This work utilizes materials which are known to exhibit definite viscoelastic effects. As explained later, our experiment is designed to minimize these effects.

Experimental Technique

A $^3/_4$-in-dia. 6061-T6 aluminum rod was machined to the configuration shown in Fig. 1. A longitudinal section $5^1/_4$ in. long and 0.373 in. high was machined from the bar. A slot 0.004 in. deep, 0.25 in. wide, and 0.3 in. long was machined in the center of the exposed surface. An EA-13-062AA-120 strain gage, with a gage length of $^1/_{16}$ in., was bonded into the slot with BR 600 adhesive. AWG No. 28 lead wires were routed to the cylindrical surface of the bar through a $^1/_{16}$-in-dia hole drilled at a 45-deg angle to the flat surface. The lead wires and strain gage were potted with BR 600 adhesive. A section 5.248 in. long and 0.371 in. high was bonded in the cutout section of the target rod with Hysol 1C epoxi-patch kit adhesive. This section was final machined to insure the continuity of the cylindrical surface. The bond line was approximately 2 mils thick; hence any impedance mismatch or viscoelastic effects from the bond were minimal. Two diametrically opposite pairs of EA-13-062AA-120 strain gages were bonded to the rod with BR 600 adhesive at the locations shown in Fig. 1. (Gage locations are identified by numbers which will be used throughout this paper.) All gage installations were cured at 170 deg F for 4 hr.

The bar was supported and aligned by two sets of adjustable screws fitted with Teflon pins. A 6061-T6 aluminum projectile 8 in. long and $^3/_4$ in. in diameter was used to impact the target rod. The projectile was fired from a gas gun capable of producing velocities from 100 to about 2000 ips [18]. For this series of tests a projectile velocity of 200 ± 5 ips was used. To insure that the projectile was not being accelerated at impact, the firing pressure was released through a vent in the gun barrel just before impact. Because alignment is so critical in this type of test, a precision-machined 3-in-long cylinder was attached to the end of the gun barrel. The diametral clearance between this cylinder and the projectile was 0.0015 ± 0.0005 in.

The projectile and target bar were aligned by observing light coming through between the contacting faces of the projectile and the target. The accuracy of alignment was checked by comparing traces from the diametrically opposite pairs of strain gages: When alignment had been performed accurately, readings from opposite gages were identical.

Preliminary tests were performed to determine the effect of the bond line in the split section of the target rod on strain-gage data traces. The solid end of the bar was impacted and the outputs from all the gages were recorded on Tektronix model 555 oscilloscopes with 1A6 preamplifiers. For the first of these tests, gages 4 and 5 were located 10 bar diameters from the impacted end, while gages 1, 2, and 3 were located about 22 bar diameters from the impact. By the time the stress pulse travels 10 bar diameters, it should be very nearly a one-dimensional stress wave. If this is in fact true, there should be essentially no change in the pulse shape from 10 bar diameters to 22 bar diameters and all gages should read the same. The sample traces, shown in Fig. 2, show the results obtained from gages 1, 2, and 4. For the first 20 microsec, all three pulses are essentially identical. Following this, the rarefaction off in the free end causes the strain pulse seen by 1 and 2 to be different from the pulse seen by 4.

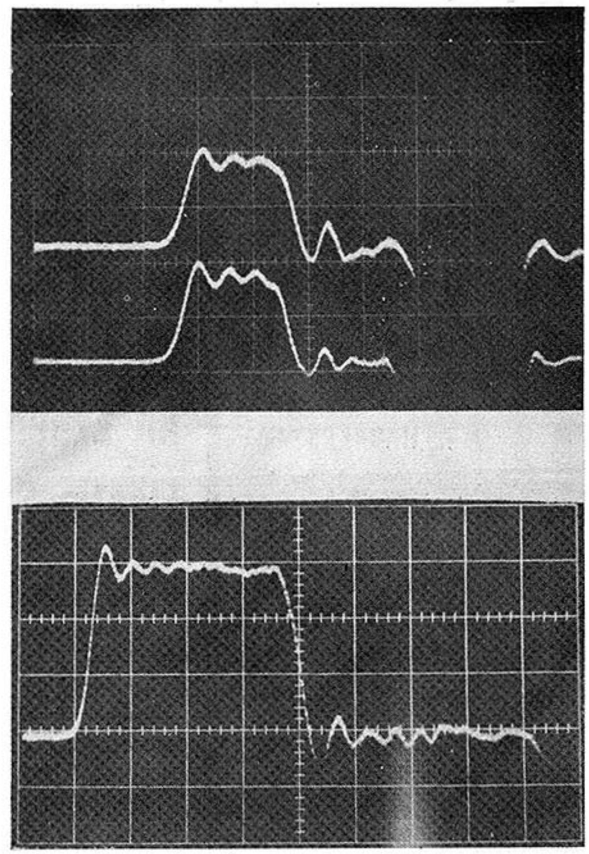

Fig. 2 Sample data traces from impact on solid end of target bar. In (a) the upper trace is gage 2 and lower trace is gage 1, both located 22 bar diameters from impact and (b) shows the record from gage 4, located 10 bar diameters from impact.

Subsequent tests were performed by impacting the split end of the bar. The distance from the gages to the impacted surface was changed by machining off appropriate portions of the bar. Fig. 3 shows sample traces from gages 1, 2, and 3 when they were located 2/3 of a bar diameter from the impact surface.

These traces show that gages 2 and 3 saw essentially the same pulse, indicating that the impact between the projectile and target bar was planar. As expected, gage 1, on the center line, shows a significantly different pulse than that obtained on surface gages 2 and 3.

Numerical Method

The TOODY1 code [12], developed by Sandia Laboratories, was utilized for all the two-dimensional calculations. This code is based upon the conservation of mass, momentum, and energy plus a constitutive relationship. In this paper, the impact velocities were maintained at such a level that the stresses remained elastic. Therefore, an isotropic, linear elastic Hooke's law was used for the constitutive relationship. The elastic properties used in the Hooke's law formulation are given in Table 1.

Table 1 Elastic constants

Dilation velocity	0.252 in/μsec
Shear velocity	0.124 in/μsec
Shear modulus	4.00 × 10^6 psi
Bulk modulus	10.65 × 10^6 psi

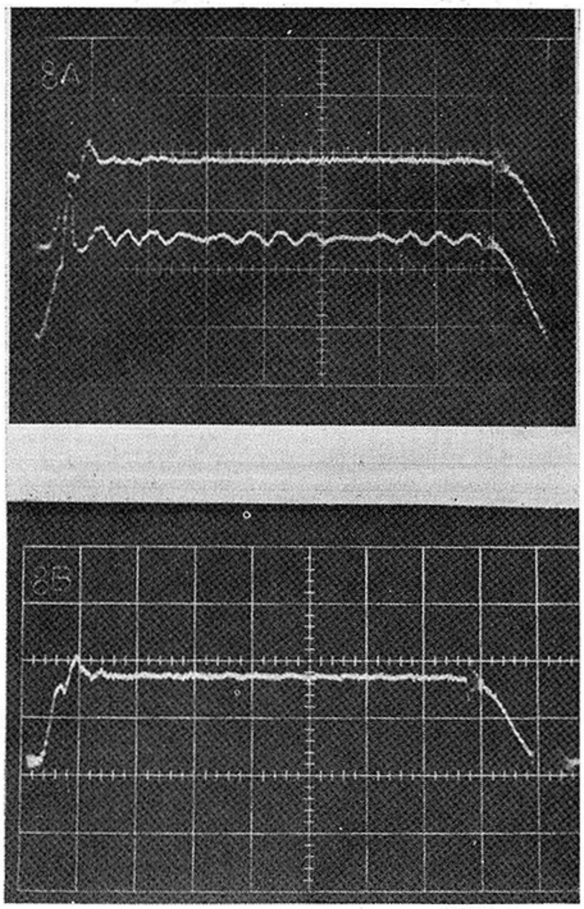

Fig. 3 Sample data traces from impact on split end of target bar. In (a) upper trace is gage 3, lower trace is gage 1. Lower photo is gage 2. All gages are located 2/3 bar diameter from impacted end.

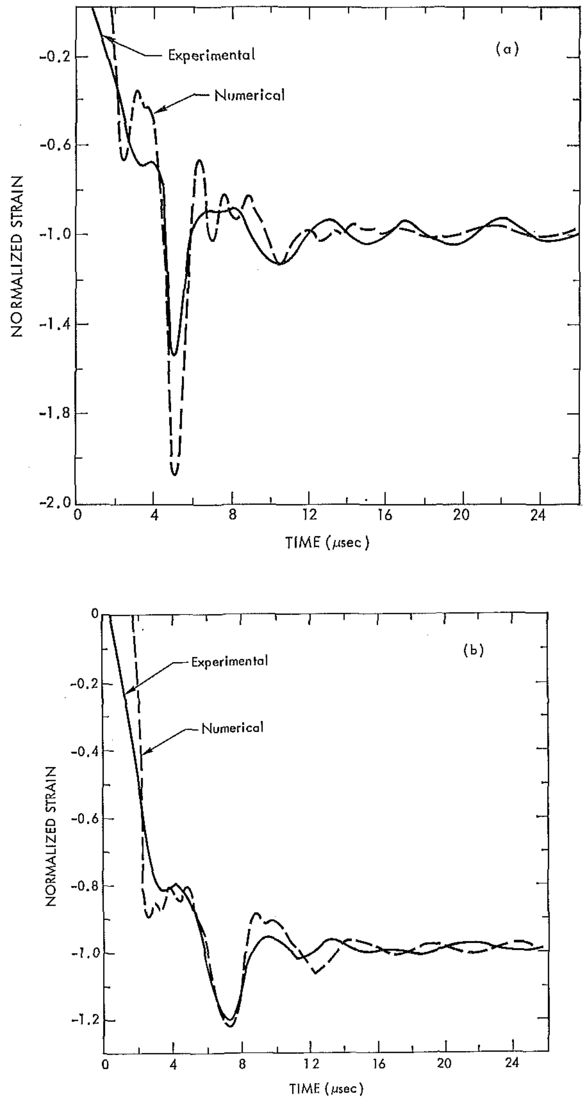

Fig. 4 Comparison of experimental and numerical results at distance of 2/3 bar diameter from impact (a) on the bar center line, and (b) on the bar surface

As noted in the Introduction, in order to stabilize the numerical scheme, it is necessary to introduce artificial viscosity terms in the manner suggested by reference [12]. The artificial viscosity form used in TOODY gives bulk and deviator components of a tensor viscosity as the sum of a quadratic and a linear term.

Much effort has been expended in studying the effect of artificial viscosity on various numerical results. For example, Hanagud, et al. [13] concluded that a large coefficient of damping could be used without affecting the results in regions removed from rapidly changing stress states, i.e., shock fronts. Bertholf [19] has found that when the deviator artificial viscosity terms in TOODY are set to zero, the code does a better job of predicting the one-dimensional state of strain that occurs on the center line and near the end of the bar before the arrival of a rarefaction wave from the free surface. This result will be further discussed in the experimental and numerical results section of this paper.

In the experiment, the striker bar collided with the target bar with some initial velocity of v_0. For calculational purposes, a Galilean transformation was performed so that the striker bar had an initial velocity to the right of $v_0/2$, while the target bar had a velocity to the left of $v_0/2$. Since this problem is strictly elastic, radial relief waves will not cause separation on the center line of the colliding bars such as was observed numerically by Karnes and Bertholf [20] and experimentally by Schuler [21]. Therefore, at the plane of collision between the two bars, i.e., $z = 0$, a symmetry condition exists which allows the grid points on this boundary to move in the radial direction (though they may not move in the axial direction). The remaining boundary conditions on the bar stipulated that there were free surfaces at $r = R$ and $z = L$.

No attempt was made to model the bond line, internal strain gage or the filled $^1/_{16}$-in-dia holes leading from the internal gage to the surface of the bar. It would require several meshes to model adequately a bond line which is approximately 0.002 in. thick. This would result in a very fine mesh system and very long running times on the computer. Also, the introduction of the bond line would destroy the axial symmetry of the problem. Hence, a three-dimensional code would be required to solve the resulting problem.

The TOODY code calculates a hoop stress. In order to determine the maximum tensile hoop stress that the adhesive bond on the split end of the bar would have to withstand, a calculation was made using the maximum projectile velocity (205 ips). The results of this calculation indicate that short-term tensile stresses up to 500 psi are generated. This is well within the tolerable stress limits for this adhesive.

Numerical and Experimental Results

The experimental axial strain records (ϵ_{zz}) on the center line ($r = 0$) and on the radial surface ($r = R$) for axial positions of $z = 0.667$, 2, and 3 bar diameters, are shown in Figs. 4–6, respectively. The solid lines give the experimental data, while the dashed lines give the numerical results computed using the TOODY code.

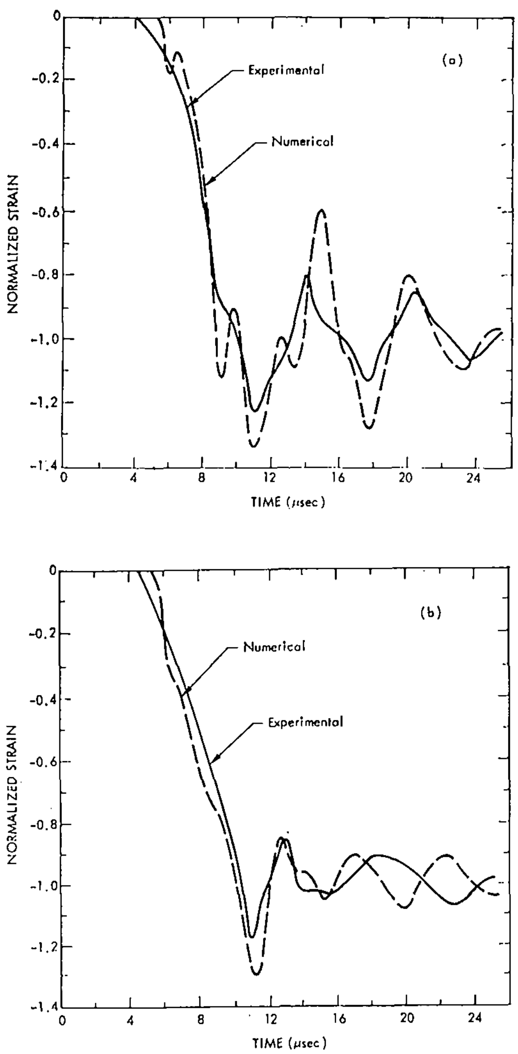

Fig. 5 Comparison of experimental and numerical results at distance of 2 bar diameters from impact (*a*) on the bar center line, and (*b*) on the bar surface

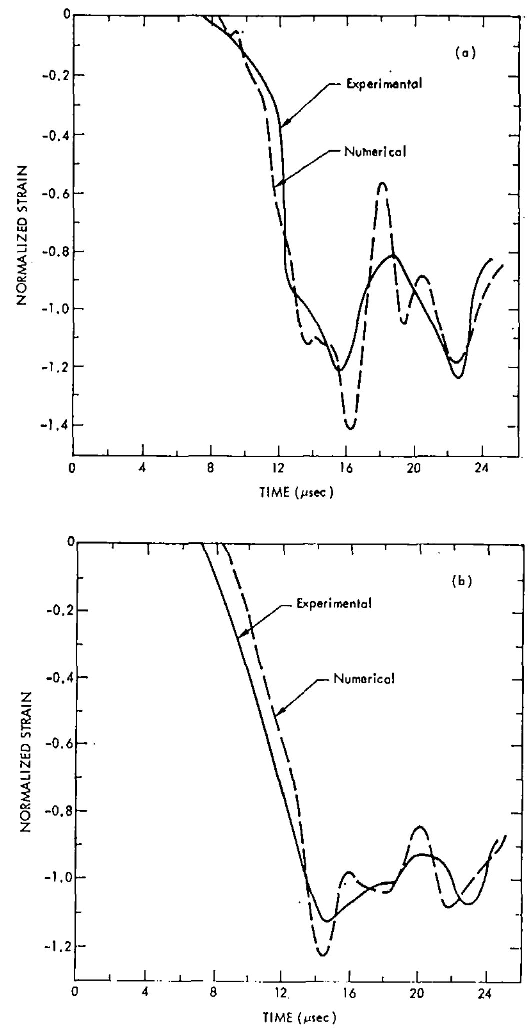

Fig. 6 Comparison of experimental and numerical results at distance of 3 bar diameters from impact (*a*) on the bar center line, and (*b*) on the bar surface

The impact velocity was adjusted in the numerical compuation so that the axial strain level predicted using elementary bar theory, i.e., one-dimensional stress, would be unity. The experimental data were normalized to unity by assuming that the stress level several microsec after the passage of the head of the pulse is equal to the elementary bar value. These assumptions are valid as long as the stresses remain elastic.

In all the numerical work shown in Figs. 4–6, 10 radial meshes were utilized (also, we chose Δz to equal Δr). We made several runs in which we utilized 20 and 30 radial zones to obtain numerical results as 2/3 bar diameters. When we compared these results to the strain gage traces, we determine that the additional computer time required for the finer meshes was not justified.

Generally the experimental and numerical results compare quite favorably. In most cases, the major features of the experimental results are reproduced by the numerical data. The procedure used in superposing the numerical and experimental results is to match the arrival times of the first significant strain peak. This results in the first strain-gage signal occurring approximately 2 microsec before the numerical scheme predicts its arrival. This discrepancy occurs in data from both the center line and the outside surface. A similar effect in surface data has been reported in references [14, 15]. The results of Koshiro Oi [22] will explain part of this effect. He determined that a realistic response time for a gage is τ = 0.5 microsec $+0.8\ L/C$ where L is the gage length and C the elementary bar speed. (For our case, τ = 0.75 microsec.) In any case, it does not seem that this effect is the result of our split-bar technique.

On the center line the numerical calculations predict the arrival of a sharp wave front traveling with the dilatational velocity. As the position of the strain record gets farther from the end of the bar, the code predicts a lower and lower amplitude for this pulse until it essentially goes to zero at three bar diameters. The experimental curve does not show as steep a rise as the numerical result. This is primarily the result of the gage system's response time. For example, the center-line gage in Fig. 4(*a*) shows a fast rise followed by a dip. The amplitude then increases to a maximum. In Fig. 5(*a*) the numerically predicted amplitude of this first sharp pulse is much lower than that observed in Fig. 4(*a*). For all of the plots, the numerically predicted peak amplitude is somewhat higher than the experimental value, but the experimental data do indicate the presence of a definite peak at the location predicted numerically.

In reference [23] numerical results on the center line of the bar at one bar diameter show sizeable oscillations for the first few microsec following the arrival of the pulse. A similar effect was noted in our elastic numerical results when the deviator artificial viscosity terms were set to zero in the TOODY code. As noted earlier, this result was confirmed through a verbal conversation with the first author of the previous paper [19]. Therefore, it is our conclusion that artificial viscosity has to be used with discretion, since the head of the pulse results can be altered significantly by the viscous terms.

Conclusion

We believe that our split-bar method for measuring internal strains gives good results in the elastic range. By using a very thin bond line, viscoelastic effects are minimized. This technique should be extended to obtain results at internal locations other than the center line, and also at locations closer to the impacted end of the bar.

Acknowledgments

The authors would like to thank G. Dittbenner for the gage installation and bonding of the aluminum bar section. We also extend our appreciation to B. Baker for his patience and meticulous care in carrying out the alignments necessary for these tests.

References

1 Pochammer, L. J. F., Math. (Creele), Bd. 81, 1876, p. 324; see Love, *The Mathematical Theory of Elasticity*, Dover Publishing Co., Inc., New York, 1944, p. 289.

2 Chree, C., "The Equations of an Isotropic Elastic Solid in Polar and Cylindrical Coordinates, Their Solution, and Application," *Transactions of the Cambridge Philosophical Society*, Vol. 25, 1889, pp. 351–360.

3 Bancroft, D., "The Velocity of Longitudinal Waves in Cylindrical Bars," *Physical Revue*, Vol. 59, 1941, pp. 588–589.

4 Davies, R. M., "A Critical Study of the Hopkinson Pressure Bar," *Transactions of the Royal Philosophical Society*, London, Series A, Vol. 240, 1948, pp. 375–457.

5 Bertholf, L. D., "Longitudinal Elastic-Wave Propagation in Finite Cylindrical Bar," Washington State University Shock Dynamics Laboratory, Pullman, Wash., Report No. 66-03, 1966.

6 Skalak, R., "Longitudinal Impact of a Semi-Infinite Circular Elastic Bar," JOURNAL OF APPLIED MECHANICS, Vol. 24, TRANS. ASME, Vol. 79, 1957, pp. 59–65.

7 Folk, R., et al., "Elastic Strain Produced by Sudden Application of Pressure to One End of a Cylindrical Bar—Experimental Observations, *Journal of the Acoustical Society of America*, Vol. 20, 1958, pp. 552–558.

8 Jones, O. E., and Norwood, F. R., "Axially Symmetric Cross-Sectional Strain and Stress Distributions in Suddenly Loaded Cylindrical Elastic Bars," JOURNAL OF APPLIED MECHANICS, Vol. 34, TRANS. ASME, Vol. 89, Series E, 1967, pp. 718–724.

9 Kennedy, L. W., and Jones, O. E., "Longitudinal Wave Propagation in a Circular Bar Loaded Suddenly by a Radially Distributed End Stress," JOURNAL OF APPLIED MECHANICS, Vol. 36, TRANS. ASME, Vol. 91, Series E, 1969, pp. 470–478.

10 van Neumann, R., and Richtmyer, R. D., "A Method of Numerical Calculation of Hydrodynamic Shocks," *Journal of Applied Physics*, Vol. 21, 1950, pp. 232–237.

11 Wilkins, M. L., "Calculation of Elastic-Plastic Flow," Lawrence Radiation Laboratory, Livermore, Report UCRL-7322, Rev. 1, 1936.

12 Thorne, B. J., and Herrmann, W., "TOODY, a Computer Program for Calculating Problems of Motion in Two Dimensions," Sandia Laboratories, Albuquerque, Report SC-RR-66-602, 1967.

13 Hanagud, S., Ross, B., and Sidhu, G., "Elastic-Plastic Impact of Plates," *Israel Journal of Technology*, Vol. 7, 1969, pp. 149–161.

14 Bertholf, L. D., "Numerical Solution for Two-Dimensional Elastic Wave Propagation in Finite Bars," JOURNAL OF APPLIED MECHANICS, Vol. 34, TRANS. ASME, Vol. 89, Series E, 1967, pp. 725–734.

15 Habberstad, J. L., "A Two-Dimensional Numerical Solution for Elastic Waves in Variously Configured Rods," JOURNAL OF APPLIED MECHANICS, Vol. 38, TRANS. ASME, Vol. 93, Series E, Mar. 1971, pp. 62–70.

16 Baker, W. E., and Dove, R. C., "Measurement of Internal Strains in a Bar Subjected to Longitudinal Impact," *Experimental Mechanics*, 1962, pp. 307–311.

17 Meitzler, A. H., "Propagation of Elastic Pulses Near the Stressed End of a Cylindrical Bar," PhD dissertation, Lehigh University, 1955, p. 52.

18 Hoge, K. G., "Behavior of Plastic-Bonded Explosives Under Dynamic Compressive Loads," *Journal of Applied Polymer Sciences*, Vol. 5, 1967, pp. 19–26.

19 Bertholf, L. D., Private communication, August 3, 1970.

20 Karnes, C. H., and Bertholf, L. D., "Numerical Investigation of Two-Dimensional, Axisymmetric Elastic-Plastic Wave Propagation Near the Impact End of Identical 1100-0 Aluminum Bars," presented at Battelle Colloquium on Inelastic Behavior of Solids, Columbus, Ohio, Sept. 1969.

21 Schuler, K. W., Sandia Laboratories, Albuquerque, private communication, August 3, 1970.

22 Oi, K., "Transient Response of Bonded Strain Gages," *Experimental Mechanics*, 1966, pp. 463–469.

23 Bertholf, L. D., and Karnes, C. H., "Axisymmetric Elastic-Plastic Wave Propagation in 6061-T6 Aluminum Bars of Finite Length," JOURNAL OF APPLIED MECHANICS, Vol. 36, TRANS. ASME, Vol. 91, Series E, 1969, pp. 533–541.